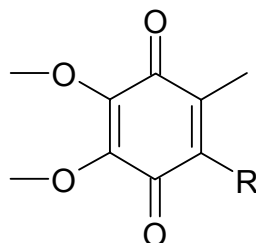


### 3. Quinones in bRC

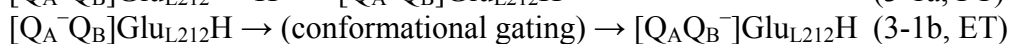
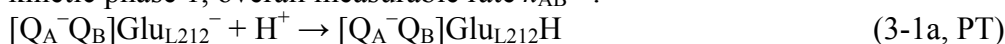
bRC possesses ubiquinone (Figure 3-0-1) as primary quinone  $Q_A$  and secondary quinone  $Q_B$ .  $Q_A$  is the electron acceptor for bacteriopheophytin on the A-branch ( $H_A$ ) as well as the electron donor to  $Q_B$ .



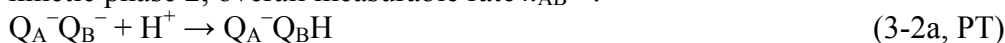
**Figure 3-0-1.** Ubiquinone. **R** stands for non-redox active part of aliphatic chain.

The coupled ET/PT reactions for  $Q_{A/B}$  in bRC proceed in two phases, as shown by the following reaction schemes (reviewed in refs. (Okamura et al., 2000; Paddock et al., 2003a)).

kinetic phase 1, overall measurable rate  $k_{AB}^{(1)}$ :



kinetic phase 2, overall measurable rate  $k_{AB}^{(2)}$ :



The PT to Glu-L212 near  $Q_B$  (see Figure 3-1-1) is a prerequisite for the first ET event belonging to kinetic phase 1 (Eq. 3-1b). In wild type bRC (WT-bRC), the rate  $k_{AB}^{(1)}$  of this kinetic phase (Eq. 3-1a,b) is independent of the ET driving-force (i.e. the  $E_m$  difference between  $Q_A$  and  $Q_B$ ). The PT rate constant belonging to kinetic phase 1 of WT-bRC was estimated to be  $10^5 \text{ s}^{-1}$  (Paddock et al., 2002). It was suggested that the ET corresponding to kinetic phase 1 is coupled to a “conformational gating” step governed by protein dynamics, which constitutes the rate-limiting step for  $k_{AB}^{(1)}$  (Graige et al., 1998). The second ET event corresponding to kinetic phase 2 (Eq. 3-2b) is coupled to a PT forming  $Q_B H$  from  $Q_B^-$  (Eq. 3-2a). This PT is governed by rate constant of  $2 \times 10^4 \text{ s}^{-1}$  (Paddock et al., 2002). In contrast to the first ET process, the rate for the second ET process depends on the driving-force, which indicates that this ET (Eq. 3-2b) is the rate-limiting step in kinetic phase 2.

#### 3.1. Conformational gating in kinetic phase 1

##### 3.1.1. Proton uptake of Glu-L212

The ET from  $Q_A^-$  to  $Q_B$  was not observed in bRC cooled in the dark, while it was observed in those cooled under illumination (Kleinfeld et al., 1984). The activation of the ET process was interpreted to be a light-induced structural change that is accompanied by protonation near  $Q_B^-$  (Kleinfeld et al., 1984). This protonation site upon formation of  $Q_B^-$  was later suggested to be Glu-L212 from the influence on  $k_{AB}^{(1)}$  upon mutation of this residues (Paddock et al., 1989; Takahashi and Wraight, 1992; Brzezinski et al., 1997).

Independently, proton uptake of Glu-L212 stoichiometrically by 0.3–0.6  $H^+$  upon

formation of  $Q_B^-$  at pH 7 has been also observed in IR (Hinerwadel et al., 1995), FTIR (Nabedryk et al., 1995), or our electrostatic computations (Rabenstein et al., 2000; Ishikita et al., 2003; Ishikita and Knapp, 2004). Molecular dynamics studies also suggested a protonation of Glu-L212 upon formation of  $Q_B^-$  (Grafton and Wheeler, 1999). We demonstrated that, even in the light-exposed structure (Stowell et al., 1997), the absence of both the proton uptake of Glu-L212 and protonated Asp-L213 renders the ET from  $Q_A^-$  to  $Q_B$  to be an energetically uphill reaction (Ishikita et al., 2003).

### 3.1.2. ET-driving force assay

The driving force assay by Graige et al. (Graige et al., 1998) confirmed the existence of conformational gating as a rate-limiting step in the ET from  $Q_A^-$  to  $Q_B$ . They replaced the ubiquinone at the  $Q_A$  binding site with exogenous quinones whose  $E_m$  differed over a range of 150 mV. Nevertheless,  $k_{AB}^{(1)}$  remained essentially unchanged, indicating that the rate-limiting step in kinetic phase 1 is not the ET but should be another process, which points to a conformational gating mechanism (Eq. 3-1b).

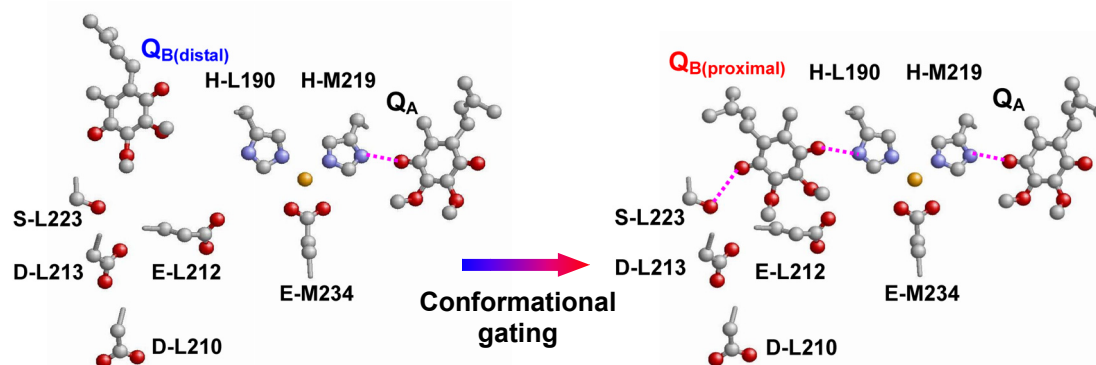


**Figure 3-1-1.**  $Q_B$  binding site of bRC from *Rb. sphaeroides*: **Left**)  $Q_B$  at the distal binding site of the dark-adapted structure (PDB 1AIJ). **Right**)  $Q_B$  at the proximal binding site of the light-exposed structure (PDB 1AIG). Possible H bonds are indicated with dotted lines.

### 3.1.3. 180° propeller twist of $Q_B$

The finding of two different  $Q_B$  positions in the crystal structures depending on whether they are obtained in the dark (the dark-adapted structure, Figure 3-1-1, left) or under illumination (the light-exposed structure, Figure 3-1-1, right) was sensational (Stowell et al., 1997).

(i)  $Q_B$  in the light-exposed structure is at a proximal binding position (relative to the Fe-complex) and  $\sim 5$  Å from that found in the dark-adapted structure (at a distal binding position), and has undergone a 180° propeller twist around the isoprene chain with respect to the dark-adapted structure.

(ii) In the light-exposed structure the carbonyl oxygen of  $Q_B$  has an additional H bond with the hydroxyl group of Ser-L223 (Figure 3-1-1, right) while this H bond is absent in the dark-adapted structure (Figure 3-1-1, left).

Thus, it was proposed that the light-induced movement of  $Q_B$  from the ET-inactive distal to ET-active proximal binding site was the origin of the conformational gating (Stowell et al., 1997). Obviously, due to the lack of an H bond between Ser-L223 and  $Q_B$  (Ishikita and Knapp, 2004), the ET from  $Q_A^-$  to  $Q_B$  in the dark-adapted structure should be energetically unfavorable with respect to the light-induced structure, indicating that this form is not relevant for the functional ET from  $Q_A^-$  to  $Q_B$  (Alexov and Gunner, 1999; Rabenstein et al., 2000; Ishikita et al., 2003).

### 3.1.4. Is the $Q_B$ movement really relevant?

If the conformational gating were controlled by the movement of  $Q_B$  (i.e.  $180^\circ$  propeller twist of  $Q_B$ ), the rate of the ET from  $Q_A^-$  to  $Q_B$  would be dependent of the length of the  $Q_B$  isoprene chain. However, the ET rate remained unchanged in those experiments (McComb et al., 1990).

In recent FTIR studies, no  $Q_B$  movement was found and both  $Q_B$  and  $Q_B^-$  are permanently located at the proximal site (Breton et al., 2002; Remy and Gerwert, 2003; Breton, 2004). Furthermore, a time-resolved crystallographic study resulted in no quinone motion upon illumination and indicated that  $Q_B$  binds only in the proximal binding site (Baxter et al., 2004). Mainly because of these experimental results that question the physiological relevance of the  $Q_B$  distal position, we prefer the light-exposed structures to describe the  $PQ_A Q_B$  and  $P^+ Q_A^- Q_B$  states, and use them consistently in the present study.

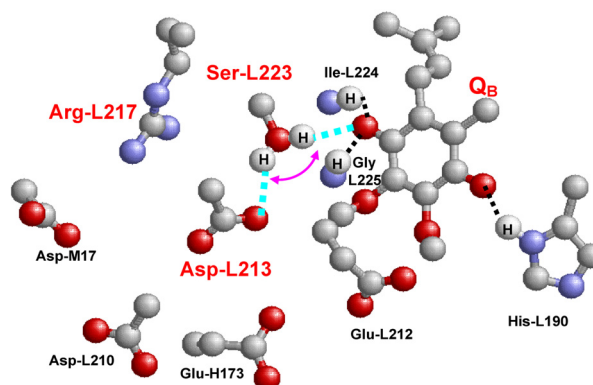


Figure 3-1-2. H-bond partners of Ser-L223.

### 3.1.5. H-bond flip of Ser-L223

Alexov and Gunner (Alexov and Gunner, 1999) found a flip of an H bond of Ser-L223 upon formation of  $Q_B^-$  in electrostatic computation based on the light-exposed structure (Stowell et al., 1997). Ser-L223 forms an H bond to the deprotonated Asp-L213, but rotates the hydroxyl H atom to the carbonyl oxygen of  $Q_B$  after the proton uptake of Asp-L213 and formation of  $Q_B^-$  state (Alexov and Gunner, 1999) (Figure 3-1-2). Recently we observed the same H-bond flip of Ser-L223 (Ishikita and Knapp, 2004) as observed by Alexov and Gunner. We found that the presence of the H bond between Ser-L223 and  $Q_B$  up-shifts the  $E_m(Q_B)$  by  $\sim 100$  mV with respect to its absence (Ishikita and Knapp, 2004). Hereby, even in the light-exposed structure, the absence of the H bond between Ser-L223 and  $Q_B$  renders the ET from  $Q_A^-$  to  $Q_B$  to an energetically uphill reaction. Thus, we proposed that the H-bond flip of Ser-L223 (i.e. rotation of the hydroxyl group from Asp-L213 to  $Q_B^-$ ) is prerequisite for the ET from  $Q_A^-$  to  $Q_B$ , as is the proton uptake of Glu-L212 (Ishikita and Knapp, 2004).

More recently, ENDOR studies suggested a significant role of Asp-L213 in the rate-limiting step for kinetic phase 1 ( $k_{AB}^{(1)}$ ) by rotating the hydroxyl group of Ser-L223 to  $Q_B^-$  (Paddock et al., 2005), as previously predicted in electrostatic computations (Alexov and Gunner, 1999; Ishikita and Knapp, 2004). For further discussion, especially for the interpretation of the kinetic phase 1, see (4.2.3).

### Conclusion:

**The conformational gating is not the movement of  $Q_B$  from the distal to proximal positions**, but smaller changes of protein conformation e.g. change of protonation pattern or H-bond pattern. We previously proposed that **an H-bond flip of**

Ser-L223 is responsible for the ET gating, in which the presence/absence of the H bond between  $Q_B$  and Ser-L223 corresponds to the ET-active/inactive conformer (Ishikita and Knapp, 2004). Recent ENDOR studies (Paddock et al., 2005) (and very recent FTIR studies (Nabedryk et al., 2005)) conformed this mechanism.

### 3.2. Varying $E_m(Q_A)$ by flip-flop H bond of Thr-M222

#### 3.2.1. H-bond pattern for $Q_A$

For bRC from *Rb. sphaeroides*, there are several crystal structures available with relatively high resolution, exhibiting variations in H-bond geometry at  $Q_A$  for His-M219/Thr-M222 with N – O / O – O distances of 4.8 Å / 2.4 Å (Chang et al., 1991), 4.4 Å / 2.8 Å (Yeates et al., 1988), 3.2 Å / 3.6 Å (Ermler et al., 1994) or 2.9 Å / 3.2 Å (Stowell et al., 1997). Based on FTIR studies for bRC, it was proposed that an H bond at  $Q_A$  fluctuates between His-M219 and Thr-M222 (Breton et al., 1994; Brudler et al., 1994). Thereby, in the  $Q_A^-$  state the 1650  $\text{cm}^{-1}$  band was significantly affected upon  $^1\text{H}/^2\text{H}$  exchange while a corresponding change in the  $Q_A^0$  state was absent. Thus, they suggested a partial shift of the H bond partner from His-M219 for  $Q_A^0$  to Thr-M222 for  $Q_A^-$  (Breton et al., 1997). The two residues are not only fully conserved among *Rb. sphaeroides*, *Rb. capsulatus* and *Bl. viridis*, but also in PSII as D2-His214 and D2-Thr217 (Figure 10-1-2).

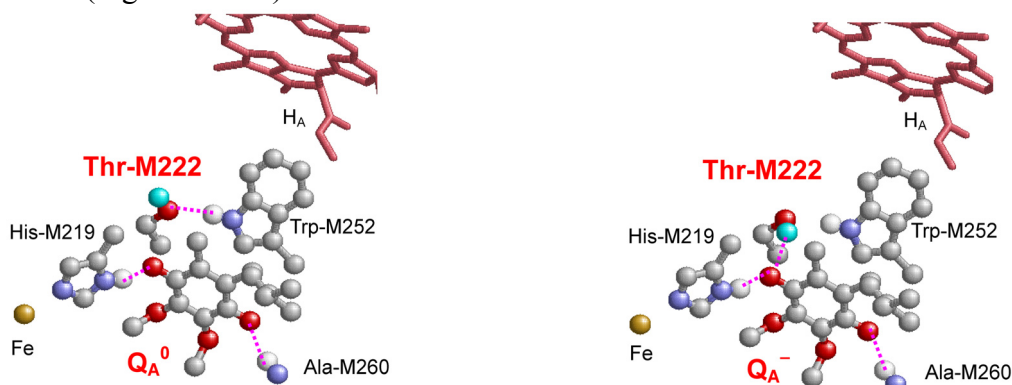


**Figure 3-2-1.** H-bond pattern of  $Q_A$  in bRC. The hydroxyl hydrogen of thr-M222 is colored in cyan. **Left)**  $Q_A^0$  state. **Right)**  $Q_A^-$  state.

#### 3.2.2. H-bond flip of Thr-M222

We found an H-bond flip of Thr-M222 upon redox change of  $Q_A$ . At the proximal carbonyl oxygen,  $Q_A^0$  possesses a single H bond with His-M219 (Figure 3-2-1, left). In this case, the calculated  $E_m(Q_A)$  was  $-170$  mV (Ishikita et al., 2003; Ishikita and Knapp, 2004, 2005e). This value is close to measured  $E_m(Q_A)$  at  $-180$  mV (Prince and Dutton, 1976; Arata and Parson, 1981). However, a higher  $E_m(Q_A)$  of  $-50$  mV has also been reported (Dutton et al., 1973). Interestingly, geometry optimization of hydrogen atoms in the  $Q_A^-$  state leads to a second H bond between the proximal carbonyl oxygen of  $Q_A$  and Thr-M222 (Figure 3-2-1, right). In agreement with our result, electrostatic computations for bRC by Zhu and Gunner (Zhu and Gunner, 2005) also implied a reorientation of the Thr-M222 hydroxyl dipole upon  $Q_A$  reduction to stabilize the negative charge. In our computation, the formation of the H bond with Thr-M222 leads to a significant up-shift of  $E_m(Q_A)$  by 130 mV (Ishikita and Knapp, 2005e). In the presence of this H bond, the computed  $E_m(Q_A)$  is  $-38$  mV (Ishikita and Knapp, 2005e), relatively high and close to the measured high-potential value of  $-50$  mV in bRC (Dutton et al., 1973). Further discussions and conclusion are given in 10.1.